

# Hot compressive deformation behavior and microstructure evolution of HIPed FGH96 superalloy

XU Wei, ZHANG Li-wen, GU Sen-dong, ZHANG Jian-lin

School of Materials Science and Engineering, Dalian University of Technology, Dalian 116024, China

Received 12 January 2011; accepted 23 July 2011

**Abstract:** Hot deformation behavior and microstructure evolution of hot isostatically pressed FGH96 P/M superalloy were studied using isothermal compression tests. The tests were performed on a Gleeble–1500 simulator in a temperature range of 1000–1150 °C and strain rate of 0.001–1.0 s<sup>-1</sup>, respectively. By regression analysis of the stress–strain data, the constitutive equation for FGH96 superalloy was developed in the form of hyperbolic sine function with hot activation energy of 693.21 kJ/mol. By investigating the deformation microstructure, it is found that partial and full dynamical recrystallization occurs in specimens deformed below and above 1100 °C, respectively, and dynamical recrystallization (DRX) happens more readily with decreasing strain rate and increasing deformation temperature. Finally, equations representing the kinetics of DRX and grain size evolution were established.

**Key words:** FGH96 superalloy; hot compressive deformation; constitutive equation; microstructure evolution; dynamical recrystallization

## 1 Introduction

FGH96 is a kind of nickle-based P/M superalloy designed by the principle of damage tolerance [1, 2]. It is mainly used in the construction of turbine disks because of its excellent properties at elevated temperature, such as good tensile and creep properties, good crack resistance and microstructure stability up to 700 °C [3, 4]. Turbine disks made from FGH96 superalloy are usually forged into shape by isothermal forging (ITF) or superplastic forging [5, 6]. However, this kind of superalloy is rather difficult to deform due to its poor work ability [7, 8]. Hence, investigation on the deformation behavior and microstructural evolution is necessary so that the processing parameters can be optimized and the microstructure can be controlled.

Several works regarding to the above two aspects have been carried out [9–11]. LIU et al [9] studied the hot deformation behavior of hot isostatically pressed (HIPed) FGH96 at 1070–1170 °C and 5×10<sup>-4</sup>–0.2 s<sup>-1</sup> by means of isothermal compression tests. LIU et al [10] did the similar work at 1000–1100 °C and 0.001–0.1 s<sup>-1</sup>, while WANG et al [11] did research at 1050–1100 °C and (0.001–0.1) s<sup>-1</sup>. These tests were carried out in relatively narrow temperature or strain rate range and

few kinetics of dynamic recrystallization for HIPed FGH96 was given. Hence, more studies are still needed.

In the present work, a set of compression tests were performed in the temperature range of 1000–1150 °C and strain rate of 0.001–1.0 s<sup>-1</sup>. From the experimental result, hot deformation behavior and microstructure evolution for HIPed FGH96 superalloy were modeled, which can give indispensable information for numerical simulation and optimizing the actual hot working processes.

## 2 Experimental

The nickle-based P/M superalloy FGH96 was produced by plasma rotation electronic pole (PREP) technology, followed by hot isostatic pressing. The chemical composition of the experimental material FGH96 is listed in Table 1. Cylindrical compression specimens with dimensions of  $d8\text{ mm}\times 12\text{ mm}$  were machined from HIPed bars. Thermo-mechanical simulation tests were conducted on a Gleeble–1500 simulator. All the specimens were first heated to the deformation temperature at a heating rate of 20 °C/s, and then isothermally compressed to a degree that true strain is equal to 1, in the temperature range of 1000–1150 °C and strain rate of 0.001–1.0 s<sup>-1</sup>. Once the compression

**Table 1** Chemical composition of FGH96 superalloy (mass fraction, %)

Cr	Co	W	Mo	Ti
15.5–16.5	12.5–13.5	3.8–4.2	3.8–4.2	3.5–3.9
Nb	Al	C	Ni	
0.6–1.0	2.0–2.4	0.02–0.05	Bal.	

test ended, the specimens were quenched in water to retain the high-temperature microstructure. Then they were sectioned and prepared for conventional microstructural observation. The grain size of the deformed specimens was measured using linear intercept method.

### 3 Results and discussion

#### 3.1 Flow stress

A set of stress—strain curves obtained from the experiment are shown in Fig. 1. It is observed that the flow stress increases rapidly to a peak in the initial stage of compression and decreases slowly to some extent as the deformation exceeds the peak strain. Finally, it goes into a steady-state region, which shows equilibrium between hardening and work softening.

Generally, plastic deformation is considered a thermally activated process and it can be described by

constitutive equations proposed by RICHARDSON et al [12]:

$$Z = \dot{\epsilon} \exp\left(\frac{Q_{\text{def}}}{RT}\right) = F(\sigma) \quad (1)$$

where  $Z$  is the Zener-Hollomon parameter;  $\dot{\epsilon}$  is the strain rate;  $R$  is the universal gas constant;  $T$  is the temperature;  $A$  is the material constant;  $Q_{\text{def}}$  is the deformation activation energy; and  $F(\sigma)$  is the function of flow stress which can be written as [13]:

$$F_1(\sigma) = A_1 \sigma^{n_1} \quad (2)$$

$$F_2(\sigma) = A_2 \exp(\beta\sigma) \quad (3)$$

$$F(\sigma) = A(\sinh(\alpha\sigma_p))^n \quad (4)$$

where  $A_1$ ,  $A_2$ ,  $A$ ,  $n_1$ ,  $n$ ,  $\beta$  and  $\alpha(\alpha=n/\beta)$  are material constants;  $\sigma_p$  is the peak flow stress. The power relationship Eq.(2) and the exponential relationship Eq.(3) are suitable for low stress level ( $\alpha\sigma < 0.8$ ) and high stress level ( $\alpha\sigma > 0.8$ ), respectively. Regarding the wide variation of flow stress in FGH96 superalloy in the present study, “hyperbolic-sine” Eq. (4) which is suitable for all the stress level is employed to model the constitutive equation.

By combining Eq. (1) with Eq. (4) and taking natural logarithm of the combination, the following

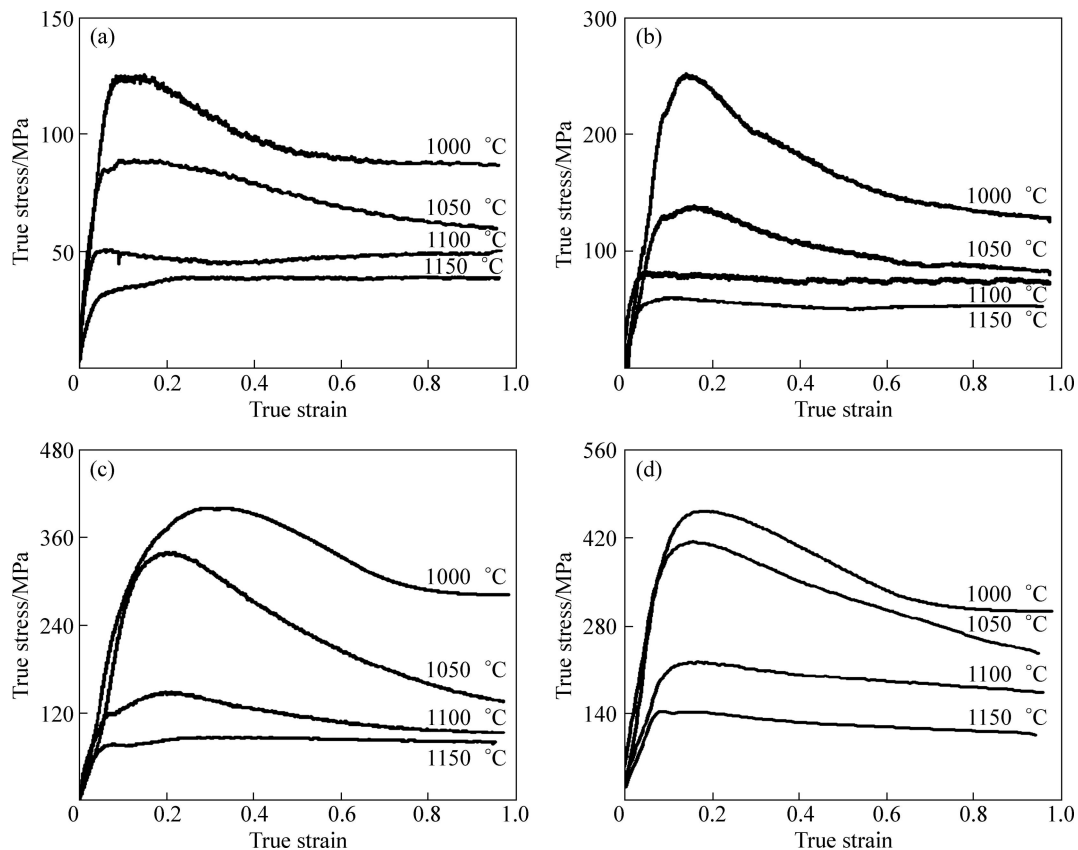


**Fig. 1** True stress—true strain curves of FGH96 superalloy during hot compression deformation: (a)  $\dot{\epsilon}=0.001 \text{ s}^{-1}$ ; (b)  $\dot{\epsilon}=0.01 \text{ s}^{-1}$ ; (c)  $\dot{\epsilon}=0.1 \text{ s}^{-1}$ ; (d)  $\dot{\epsilon}=1.0 \text{ s}^{-1}$

equation can be obtained:

$$\ln \dot{\epsilon} + \frac{Q_{\text{def}}}{RT} = \ln A + n \ln(\sinh(\alpha \sigma_p)) \quad (5)$$

In Eq. (5),  $n$  represents the slope of  $\ln(\sinh(\alpha \sigma_p))$  versus  $\ln \dot{\epsilon}$ , as shown in Fig. 2(a). As a material constant, it is independent on temperature. Hence, an appropriate value for  $\alpha$  is required and an iterative scheme is adopted to achieve this, namely, different value for  $\alpha$  is generated until  $n$  values under different deformation conditions approximately reach the same value[14]. It is calculated that for the value of  $\alpha=0.004$ ,  $n$  is almost independent on temperature and its mean value is equal to 4.14.

Figure 2(b) shows the dependence of peak stress on temperature. By utilizing the linear relationship between natural logarithm of  $\sigma$  versus  $1/T$ , the deformation activation energy  $Q_{\text{def}}$  is determined to be 693.21 kJ/mol.

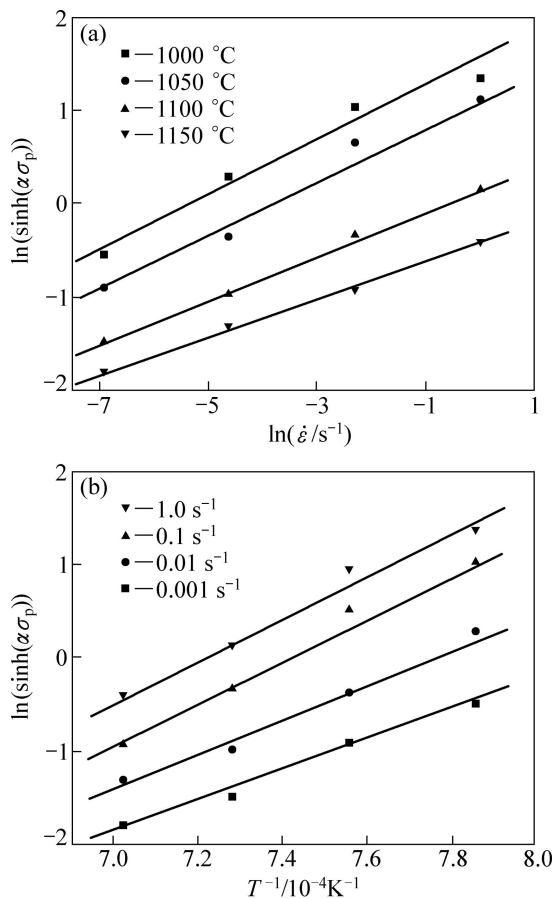


**Fig. 2** Dependence of peak stress on strain rate (a) and temperature (b)

Table 2 summarizes all the calculated constants in Eq. (5). By substituting the values into Eq. (1), the equation for peak deformation stress as a function of  $Z$  is as follows:

$$\sigma_p = 227 \sinh^{-1}(2.40 \times 10^{-25} Z)^{0.24} \quad (6)$$

**Table 2** Measured constants for FGH96 superalloy

$Q_{\text{def}}/(kJ \cdot mol^{-1})$	$\alpha/MPa^{-1}$	$n$	$\ln(A/s^{-1})$
693.21	0.004	4.14	60.20

### 3.2 Microstructure observation

Figure 3 shows the typical optical micrograph of HIPed FGH96 superalloy before deformation. In the specimens, round previous particle boundaries (PPBs) can be seen, along which no DRX grains appear. This indicates that the powder particles with diameter of 50–100  $\mu m$  are hardly deformed during the HIP process. Inside the particles, there is quite a lot of primary  $\gamma'$ , and the morphology of grains is difficult to distinguish.

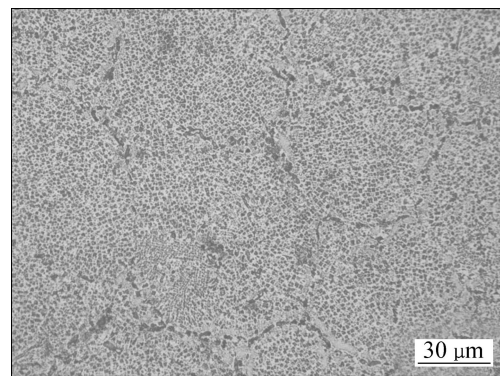


**Fig. 3** Initial microstructure of HIPed FGH96 superalloy

After deformation, microstructures recorded in the central region of the specimens are observed. Figure 4 shows the microstructure of FGH96 superalloy deformed at lower temperature and the compression axis is vertical. It can be seen that a large amount of  $\gamma'$  still exists in the microstructure; PPBs are redistributed due to deformation and are difficult to distinguish. However, by the local distribution of  $\gamma'$ , it can be noticed that previous particles (marked by the arrows) are elongated along the direction perpendicular to the compression axis. At higher magnifications, some new grains are observed. These grains mainly appear along the PPBs and only a small fraction can be found. The appearance of these new small grains indicates the occurrence of partial dynamical recrystallization (DRX).

When the deformation temperature exceeds 1100 °C, most  $\gamma'$  has been dissolved and new recrystallized grains are ubiquitous (Fig. 5), which means that DRX has taken place almost completely. Therefore, it is concluded that the deformation temperature strongly affects the DRX behavior of FGH96 superalloy and DRX is more readily to happen at higher temperatures. Similarly, the DRX grain size is also affected by deformation temperature and strain rate. The metallographic observation indicates that in the full DRX region, grain size increases with increasing deformation temperature and decreasing strain rate. More details about the effect of deformation

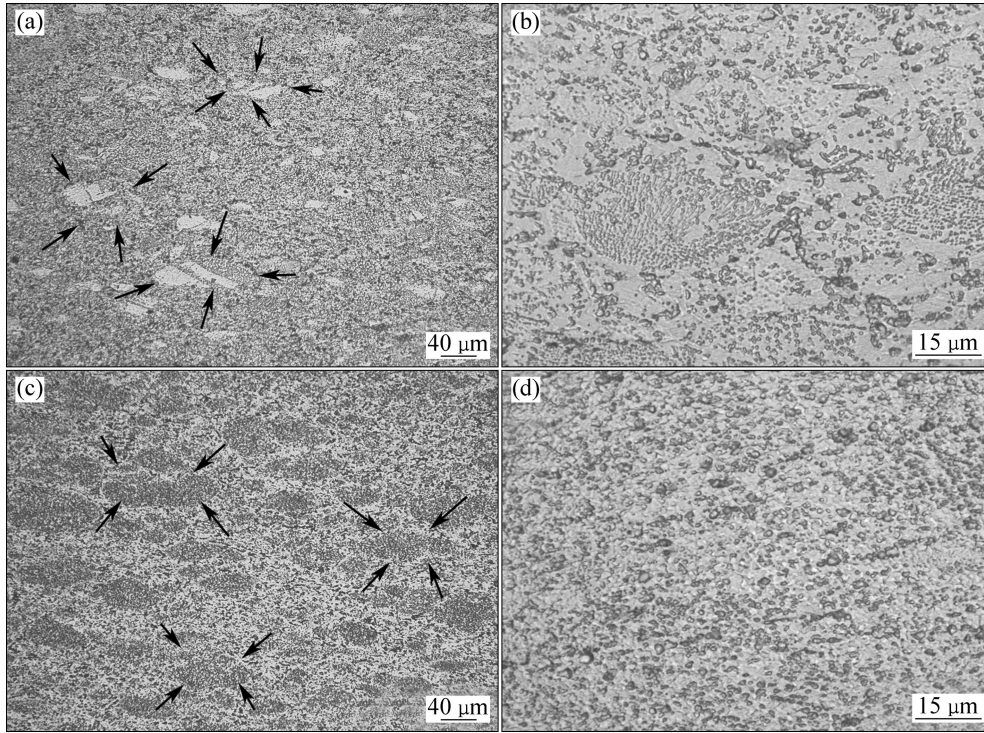


**Fig. 4** Microstructure of FGH96 superalloy deformed at 1000 °C, 0.01 s<sup>-1</sup> (a, b) and 1050 °C, 1.0 s<sup>-1</sup> (c, d)

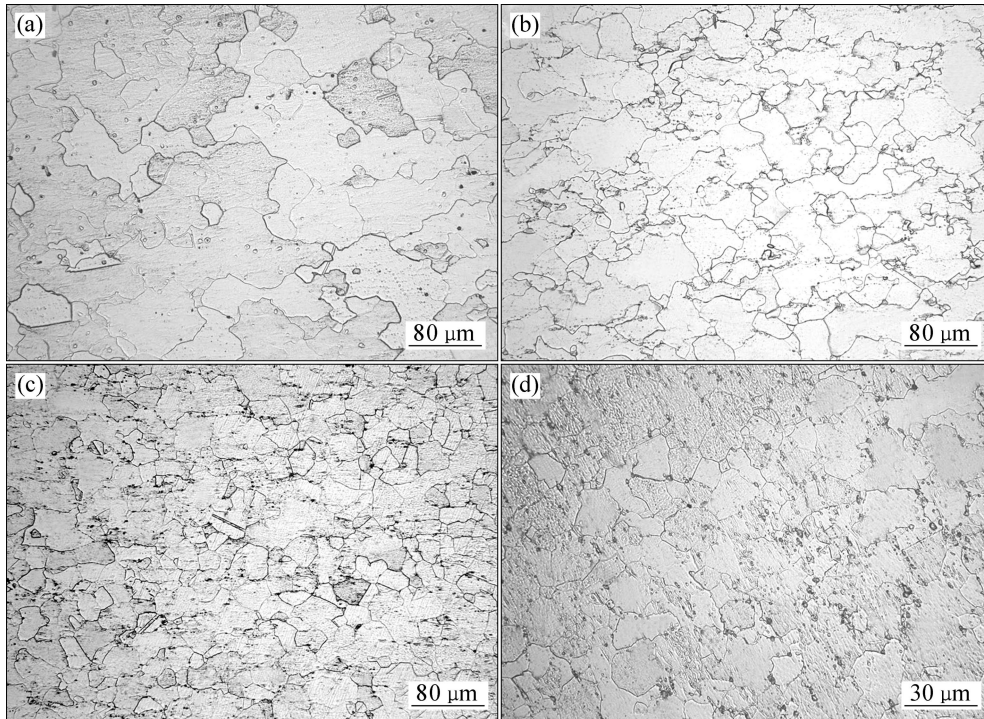


**Fig. 5** Microstructures of FGH96 deformed at 1150 °C: (a)  $\dot{\epsilon}=0.001 \text{ s}^{-1}$ ; (b)  $\dot{\epsilon}=0.01 \text{ s}^{-1}$ ; (c)  $\dot{\epsilon}=0.1 \text{ s}^{-1}$ ; (d)  $\dot{\epsilon}=1.0 \text{ s}^{-1}$

temperature and strain rate on microstructural evolution mechanism are needed to study in further investigations.

### 3.2.1 Kinetics of dynamic recrystallization

DRX is a time-dependent process. Isothermal DRX kinetics measured in hot working experiments is usually described by the Avrami equation [15, 16]:

$$X_{\text{dyn}} = 1 - \exp[-\ln 2(t/t_{0.5})^2] \quad (7)$$

where  $X_{\text{dyn}}$  is the dynamically recrystallized fraction,  $t$  is the time after the start of DRX and  $t_{0.5}$  is the time for 50% recrystallization which is expressed as:

$$t_{0.5} = A\dot{\epsilon}^b \exp(Q/T) \quad (8)$$

where  $A$ ,  $b$  and  $Q$  are constant.

The following method is employed to achieve  $t_{0.5}$  under each deformation condition. First, the softening fraction is given as [17]:

$$X_{\text{dyn}} = \frac{\sigma^p - \sigma}{\sigma^p - \sigma_s^{\text{dx}}} \quad (9)$$

where  $\sigma_s^{\text{dx}}$  is the steady flow stress obtained from the stress—strain curves.

Through Eq. (9), the stress for 50% recrystallization can be calculated. Then, the corresponding strain can be obtained from the stress—strain curves and divided by strain rate to get time for 50% recrystallization. Figures 6 and 7 show the variation of  $t_{0.5}$  with respect to temperature and strain rate, respectively.

When  $t_{0.5}$  is available, its dependence on deformation condition ( $\dot{\epsilon}$ ,  $1/T$ ) can be gained by multiple linear regressions. The result with an  $R$ -square value of about 0.98 is given as

$$t_{0.5} = 4.57 \times 10^{-3} \dot{\epsilon}^{-0.88} \exp(6.36 \times 10^3 / T) \quad (10)$$

### 3.2.2 Dynamically recrystallized grain size

As mentioned above, the dynamically recrystallized

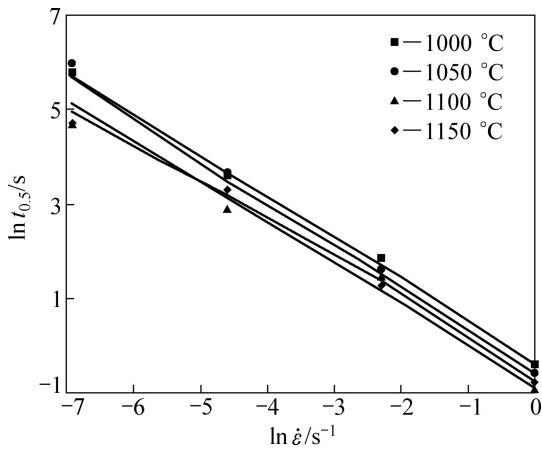


Fig. 6 Relationship between  $t_{0.5}$  and strain rate at different temperature

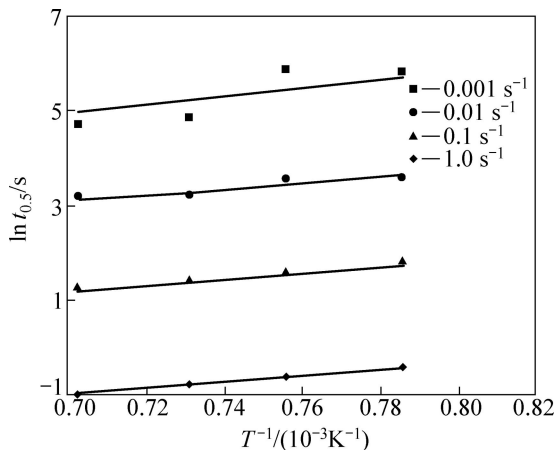


Fig. 7 Relationship between  $t_{0.5}$  and temperature at different strain rate

grain size is dependent on temperature as well as strain rate, and this dependence can be described by only one  $Z$  parameter. The larger the  $Z$  is, the more the energy is stored due to deformation. Correspondingly, the driving force for DRX grows large and the refinement of dynamically recrystallized grain size becomes easy. The dependence of dynamically recrystallized grain size on  $Z$  can be written as [18]:

$$D_{\text{dyn}} = CZ^{-n_D} \quad (11)$$

where  $C$  and  $n_D$  are the experimental constants.

In all fully recrystallized specimens, dynamically recrystallized grain size under each deformation condition is collected by quantitative metallography method. The natural logarithm of  $D_{\text{dyn}}$  versus that of  $Z$  for the specimens deformed at 1100 and 1150 °C with strain rate from 0.001 to 1.0  $\text{s}^{-1}$  is plotted in Fig. 8. By linear fitting, the relationship between the two parameters is determined as:

$$\text{Ln } D_{\text{dyn}} = -0.22 \text{Ln } Z + 15.21 \quad (12)$$

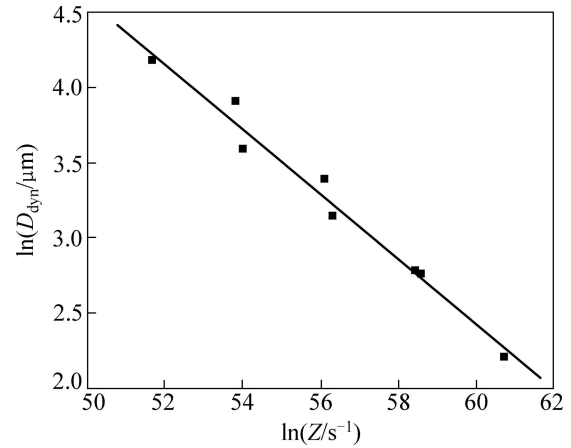


Fig. 8 Relationship between  $D_{\text{dyn}}$  and  $Z$

## 4 Conclusions

1) The flow stress behavior of FGH96 superalloy is temperature- and strain rate-sensitive. As the temperature and strain rate decrease, the peak stress decreases. The logarithm of peak stress shows good linearity with that of strain rate or the inverse temperature. By regression analysis, activation energy  $Q_{\text{def}}$  and stress exponent  $n$  for FGH96 superalloy are determined to be 693.21 kJ/mol and 4.14, respectively.

2) The occurrence of partial or full DRX behavior can be observed below or above 1100 °C, respectively. The fraction of DRX is determined by the Avrami equation.

3) The dependence of grain size on the deformation condition can be described by only one parameter  $Z$ .

## References

- [1] The Editorial Board of China Aeronautical Materials Handbook. China aeronautical materials handbook [M]. Beijing: Standards Press of China, 2002: 44–47. (in Chinese)
- [2] GUO Wei-min, DONG Jian-xin, WU Jian-tao, ZHANG Feng-ge, CHEN Gan-sheng, CHEN Sheng-da. Microstructure and properties of PM superalloys FGH96 [J]. Journal of Iron and Steel Research, 2005, 17(1): 59–64. (in Chinese)
- [3] WANG Wu-xiang, HE Feng, ZOU Jin-wen. The application and development of P/M superalloys [J]. Journal of Aviation Engineering and Maintenance, 2002(6): 26–28. (in Chinese)
- [4] REED R C. The superalloys: Fundamentals and applications [M]. Cambridge University Press, 2006: 236–274.
- [5] PARK N K, KIM I S, NA Y S, YEOM J T. Hot forging of nickel-base superalloys [J]. Journal of Materials Processing Technology, 2001, 111(1–3): 98–102.
- [6] WANG Xu-qing, LUO Xue-jun, ZOU Jin-wen. Effect of HIP temperature on microstructure of FGH96 superalloy [J]. Journal of Aeronautical Materials, 2006, 26(3): 293–294. (in Chinese)
- [7] NING Y Q, YAO Z K, GUO H Z, FU M W, LI H, XIE X H. Investigation on hot deformation behavior of P/M Ni-base superalloy FGH96 by using processing maps [J]. Material Science and Engineering A, 2010, 527(26): 6794–6799.
- [8] ZHANG Ren-peng, LI Fu-guo, WANG Xiao-na. Determining processing maps of FGH96 superalloy [J]. Journal of Northwestern Polytechnical University, 2007, 25(5): 652–656. (in Chinese)
- [9] LIU Jian-tao, LIU Guo-quan, HU Ben-fu, SONG Yue-peng, QIN Zi-ran, ZHANG Yi-wen. Hot deformation behavior of FGH96 superalloy [J]. Journal of University of Science and Technology Beijing, 2006, 13(4): 319–323.
- [10] LIU Yu-hong, LI Fu-guo, YU Hong-bo. Deformation behavior of hot isostatic pressing FGH96 superalloy [J]. Transactions of Tianjin University, 2006, 12(4): 281–285.
- [11] WANG Xiao-na, LI Fug-uo, LIU Yu-hong. Deformation and microstructural evolution in alloy FGH96 under isothermal forging condition [J]. Powder Metallurgy Technology, 2008, 26(3): 196–200. (in Chinese)
- [12] RICHARDSON G J, SELLARS C M, TEGART W J M. Recrystallization during creep of nickel [J]. Acta Metallurgica, 1966, 14(10): 1225–1236.
- [13] RAO K P, HAWBOLT E B. Development of constitutive relationships using compression testing of a medium carbon steel [J]. Journal of Engineering Materials and Technology, 1992, 114(1): 116–123.
- [14] SALEHI A R, SERAJZADEH S, YAZDIPOUR N. A study on flow behavior of A-286 superalloy during hot deformation [J]. Materials Chemistry and Physics, 2007, 101(1): 153–157.
- [15] JONAS J J, QUELENNEC X, JIANG L, MARTIN É. The Avrami kinetics of dynamic recrystallization [J]. Acta Materialia, 2009, 57(9): 2748–2756.
- [16] LORIA E A, DETERT K, MORRIS J G. On the Avrami analysis of dimensionality in recrystallization [J]. Acta Metallurgica, 1965, 13(8): 929–931.
- [17] YUE Chong-xiang, ZHANG Li-wen, LIAO Shu-lun, PEI Ji-bin, GAO Hui-ju, JIA Yuan-wei, LIAN Xiao-jie. Research on the dynamic recrystallization behavior of GCr15 steel [J]. Material Science and Engineering A, 2007, 499(1–2): 177–181.
- [18] MEDINA S F, HERNANDEZ C A. Modelling of the dynamic recrystallization of austenite in low alloy and microalloyed steels [J]. Acta Materialia, 1996, 44(1): 165–171.

## 热等静压态 FGH96 合金的热压缩变形行为和 微观组织演化

徐伟, 张立文, 顾森东, 张建新

大连理工大学 材料科学与工程学院, 大连 116024

**摘要:** 通过热压缩实验研究热等静压态 FGH96 合金的热变形行为和微观组织演化过程。基于 Gleeble-1500, 在 1000~1150 °C 和 0.001~1.0 s<sup>-1</sup> 的条件下进行热压缩实验。对应力—应变数据进行拟合分析, 建立 FGH96 合金的双曲正弦函数形式的本构关系, 其形变热激活能为 693.21 kJ/mol。对各变形条件下的 FGH96 合金的组织分析表明: 在 1100 °C 以上和以下分别发生完全和部分动态再结晶, 在高变形温度和低应变速率条件下动态再结晶更容易发生。建立 FGH96 合金在热加工过程中的动态再结晶的动力学方程和晶粒尺寸演化方程。

**关键词:** FGH96 合金; 压缩变形; 本构方程; 组织演化; 动态再结晶

(Edited by FANG Jing-hua)